Int. J. Microgravity Sci. Appl., **36** (4) (2019) 360401
DOI: 10.15011//jasma.36.360401

IIII Review IIII

A Review of Pool Boiling in Superfluid Helium under Microgravity Condition

Suguru TAKADA

Abstract

This review is intended to summarize the status and the open issues in the studies of boiling in saturated superfluid helium under microgravity condition. Superfluid helium has been utilized even in microgravity for cooling detectors and mirrors onboard satellites. Superfluid helium is called a quantum fluid that has many characteristic features. The heat transfer mechanism in superfluid helium due to internal convection is much different from that in ordinal fluid even in microgravity. In this review paper, the fundamental properties of superfluid and the effect of gravity upon boiling in superfluid helium will be described, and several microgravity experiments results will be reviewed. To conclude, the several numerical studies and some open issues will be summarized.

Keyword(s): Microgravity, Superfluid helium, Boiling, Vapor bubble, Visualization
Received 30 August 2019, accepted 7 October 2019, published 31 October 2019.

Nomenclature

a van der Waals constant for helium 3.45 x 10^{-3} Pa m^6/mol^2
D diameter (m)
g gravity acceleration (m/s^2)
h_{fg} latent heat (J/kg)
j mass flux density across vapor-liquid interface (kg/m^2)
K_{GM} constant value 11.3
m_{He4} molecular mass of helium 4.0026 g/mol
Δp_{vdW} van der Waals pressure (Pa)
q heat flux (W/m^2)
q_w heat flux at wall (W/m^2)
q_i heat flux at vapor -liquid interface (W/m^2)
q_{cr} critical heat flux of onset film boiling (W/m^2)
$q_{c\infty}$ calculated critical heat flux by Zuber's equation(W/m^2)
Q total heat input (W)
Q_i total heat flow across vapor-liquid interface (W)
R_{He} the gas constant for helium 2,097 (J/kg K)
R radius (m)
R' normalized radii
s entropy (J/kg K)
T temperature (K)
T_b temperature of superfluid helium bath (K)
T_i temperature at vapor-liquid interface (K)
ΔT_{sub} subcooling (K)

Greek letters

β thermal condensation coefficient
φ emperical parameter
η_n viscosity of normal fluid component (Pa s)
ρ total density of superfluid helium (kg/m^3)
ρ_s density of superfluid component (kg/m^3)
ρ_n density of normal fluid component (kg/m^3)
ρ_v density of vapor (kg/m^3)
ρ_l density of liquid (kg/m^3)
σ surface tension (Pa/m)

1. Introduction

Liquid helium of Helium 4 has two phases as shown in **Fig. 1**. The lower temperature phase below approximately 2.17 K is called Superfluid Helium or He II. He II is a quantum fluid of which its appearance can be explained on the basis of quantum mechanics theory of Bose-Einstein condensation. Another isotropic form of Helium 3 also has a superfluid phase in liquid state. However, superfluid phase of Helium 3 only appears below a few milli-kelvin. In this paper, only superfluid helium in Helium 4 (He II) is described.

He II has many unique features that are significantly different from those of ordinary fluids. The most important feature for He II boiling is extremely high effective thermal conductivity. The unique feature is explained on the basis of the Landau's two-fluid model. According to the model, He II is assumed to be a mixture of the normal fluid and the superfluid components. The total

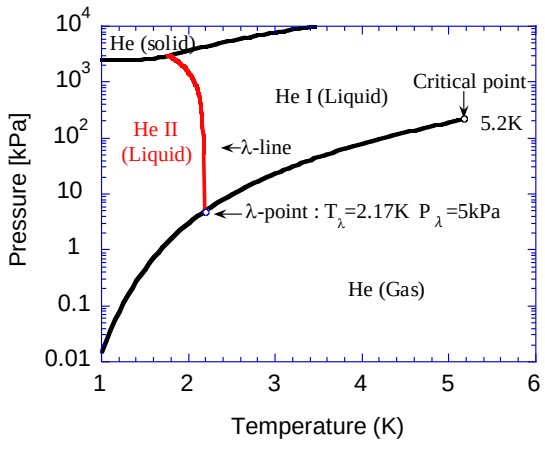

Fig. 1 Phase diagram of ^{4}He.

National Institute for Fusion Science, 322-6 Oroshi-cho, Toki, Gifu 509-5292 Japan.
(E-mail: takada.suguru@nifs.ac.jp)

density is expressed as the total sum of each component as,

$$\rho = \rho_s + \rho_n \quad (1)$$

where ρ_s and ρ_n are the densities of the superfluid component and the normal component. The superfluid component has no entropy and no viscosity. On the other hand, the normal fluid component has non-zero entropy and viscosity. The fraction of densities between the two components are shown in **Fig. 2**.

The two components move in the opposite direction when temperature rise appears. This internal flow is called the thermal counter flow or fountain effect. Thermal counter flow is caused by the difference in the chemical potential resulting from temperature difference. When the temperature rises at one side of a channel, the superfluid component flows in the direction of the higher temperature side and the normal component flows to the opposite side. This thermal counter flow can realize extremely high effective thermal conductivity. In the case of He II, natural convection due to buoyancy effect is negligibly small. Thus, the effect of gravity to heat transfer in He II is rather small.

As a result of its high ability for heat transport, He II was applied to cooling superconducting magnets for various advanced projects such as a high energy accelerator, nuclear magnetic resonance (NMR) spectrometer of very high magnetic fields and a fusion reactor [1–6].

He II in microgravity has been also utilized for scientific satellite missions. For example, detectors on space satellites have been cooled with He II in Infrared telescopes and x-ray telescope [7, 8]. For these space missions, many microgravity experiments had been carried out by using parabolic flights and sounding rockets [9-14]. In these He II applications in space, He II has not experienced rather large heat load. He II only plays the role of maintaining a constant temperature bath. Thus, the many investigations of phase separation and behavior of film flow were reported but the boiling experiments were few [15-17]. For normal liquid helium (He I), the studies of microgravity experiments are also few [15]. The study of boiling heat transfer in He II should be important knowledge for designing future challenging applications that require larger heat transport in He II.

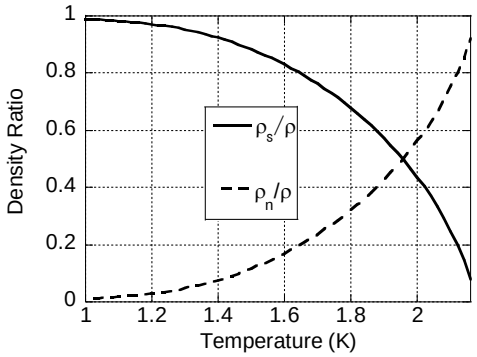

Fig. 2 Density ratios of the superfluid component and the normal fluid component with respect to the total density.

Recently, the requirement for cooling detectors is growing higher and the mechanical cooler for low temperature is also improved. Thus, the role of He II application should be changing to heat transport device or thermal storage. In other words, the heat transfer with large heat load should be investigated to further He II applications.

2. Effect of Gravity on He II Boiling

In He II, steady nucleate boiling state is absent because vapor bubbles cannot exist due to extremely high heat transport capability. Thus, the film boiling without detached bubbles exists in He II. The several film boiling modes were found depending on the pressure (i.e., subcooling) as shown in **Fig. 3** [18, 19]. Under nearly saturated vapor pressure condition, the immersion depth of about 20 cm is generally the border between the noisy and the silent film boiling modes [20]. These vapor behaviors of the two film boiling modes are significantly different as shown in **Fig. 4** and **Fig. 5**. In the silent film boiling mode, vapor film is stable, and the interface looks smooth. On the other hand, in the noisy film boiling mode, the vapor repeated generation and collapse accompanying with audible loud noise and harmful mechanical vibration. The transition between the noisy film boiling and the silent film boiling in saturated He II is easily observed in an experimental set up equipped with a movable rod as shown in **Fig 6**. The bath temperature is controlled by a valve and a vacuum pump. The hydrostatic pressure is controlled by changing immersion depth of test section.

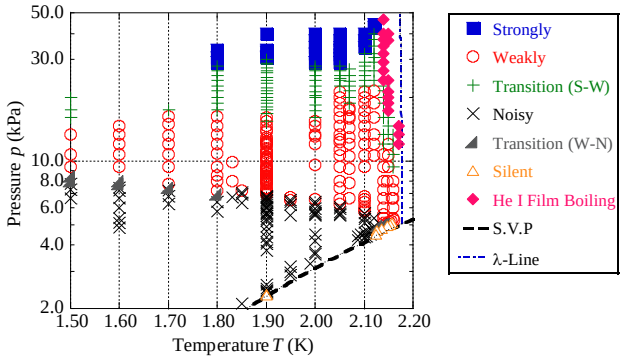

Fig. 3 Film boiling map in He II on phase diagram[18].

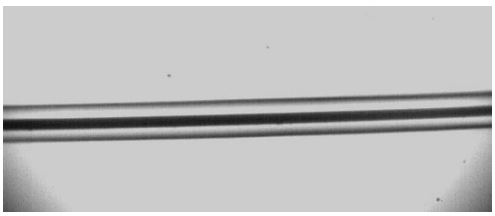

Fig. 4 Typical visualization results of the silent film boiling around wire heater of 50 micron manganin in saturated He II at 1.9 K, Immersion depth 10 cm, q_w = 8.929 W/cm^2 [20].

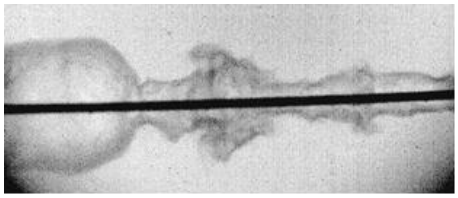

Fig.5 Typical photograph of the noisy film boiling around wire heater, $T_b = 2.02$ K, $q_w = 19.6$ W/cm^2. Immersion Depth 20 cm [20].

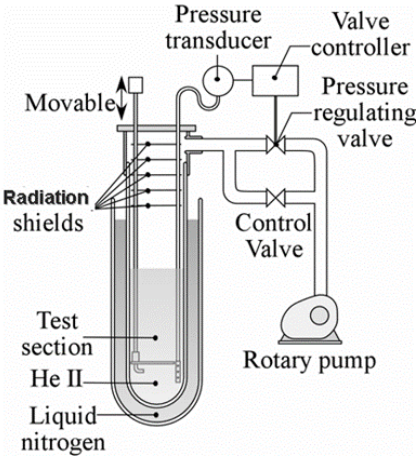

Fig. 6 Schematic illustration of a typical experimental set up of saturated He II in glass Dewar.

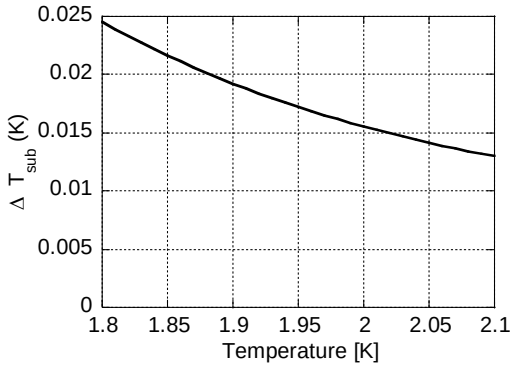

Fig. 7 The subcooling due to the hydrostatic pressure head of the small immersion depth of 10 cm.

Figure 7 shows the subcooling of temperature difference as a function of hydrostatic pressure heads between the immersion depth of only 10 cm and the free surface. The subcooling is only a few milli kelvin, however, the ratio, $\Delta T_{subcool} / T_{sat}$, is significantly large because He II is low temperature liquid. The heat transport was explained by minute subcooling [1]. Therefore, the pressure head plays a significant role in He II and the microgravity experiment is required.

3. Peak Heat Flux (Onset of Film Boiling)

The first microgravity experiment of He II boiling was carried out by Gradt, et. al., [16]. In the experiment, the low gravity environment had been realized onboard a parabolic flight of a NASA KC-135 aircraft. The thin heater wire of 20 micron was used because the maximum electric current was limited on account of external requirements of the flight apparatus. The length of the wire heater was about 20 mm. The heater current was supplied in the form of a triangle shape in 10 seconds under below 25 mG condition. In this experiment, the onset heat flux and the recovery heat flux were measured. And the authors predicted that compared with ground experiments, the magnitude of the peak heat flux was successfully explained by taking the van der Waals force between the heater surface and He-atoms into account in the case of microgravity. Another ground experiment supported that consideration independently [21]. However, the flight experiment had been conducted at only one temperature condition and the data had largely scattered data due to the limitation of a parabolic flight experiment such as the time duration and the vibration condition. The authors considered the model on the basis of linear relationship on the hydrostatic pressure, but rather large scattered data of the recovery heat flux could not be recognized linear [16]. All scattered data were spread below the prediction on the basis on the kinetic theory from the correlation from ground experiments.

Another approach of microgravity experiment had been carried out after the above experiment by using the drop tower [22-24]. The 10 m-drop tower at Hokkaido center of AIST (National Institute of Advanced Industrial Science and Technology) can provide microgravity environment below 1 mG for approximately 1.3 sec. The drop tower is a double capsule type in open atmosphere so that it has the advantage that repetitive experiments can be easily carried out while changing experimental conditions. Even more than several ten experiments per day can be conducted. Because of the short time duration of microgravity, a constant heat flux was applied from start to finish. The wire diameters of 50 μm and 80 μm and the length of approximately 40 mm had to be selected because of the requirements of the drop tower. Thus, the results cannot be strictly compared with the parabolic flight. The rather large diameters were selected in order to clarify the effect of the surface tension and Van der Waals force. The temperature dependence was also investigated.

The effect of Van der Waals pressure to the onset of boiling was confirmed from these data. **Figure 8** shows the dependence of peak heat flux on hydrostatic pressure. The peak heat fluxes have a linear correlation with the hydrostatic pressure head for the two wires. And the offset pressure is about 80 Pa independently on the wire diameter. Van der Waals pressure can be expressed as,

$$\Delta p_{vdW} = \left(\frac{\rho_v}{m_{He4}} \right)^2 \cdot a \qquad (2)$$

When the bath temperature of He II is 1.9 K, the van der Waals pressure is about 76.5 Pa. **Figure 9** shows temperature dependence which indicates the calculation taking into account that van der Waals force can explain experimental results. The peak heat flux can be calculated by using the extended Gorter-Millink equation, which is a fundamental equation to express steady heat transfer. Gorter-Millink equation is,

$$\nabla T = f(T)\cdot q^m \ , \quad f(T) = \frac{A_{GM}\rho_n}{\rho_s^3 s^4 T^3} \tag{3}$$

where A_{GM} is Gorter-Millink coefficient, and constant value m = 3.4. The entropy is referred from the table of the helium properties under saturated vapor pressure condition. The Gorter-Millink coefficient, A_{GM}, were calculated by the Soloskii's correlation (4)[25].

$$A_{GM} = \frac{1}{K_{GM}}\frac{\rho}{\rho_s \eta_n} \tag{4}$$

The integration of equation (3) and (4) over the temperature difference in account to van der Waals pressure with Clausius-Clapeyron approximation yields the peak heat flux as follows.

$$q_{cr} = \left(\frac{(m-1)\varphi}{r} \cdot \frac{T_b}{\rho_v h_{fg}} \cdot \frac{\Delta p_{vdW}}{f(T_b)} \right)^{1/m} \tag{5},$$

Here unfortunately the empirical parameter $\varphi = 0.2$ is included. The value 0.2 is found to be almost consistent among the past researches[1]. These empirical values have not been understood yet. That is not only related to the wire radius but also to the pressure of He II bath [1].

In addition, the boiling heat transfer in normal liquid helium (He I) under atmospheric pressure condition was also tested [24]. **Figure 9** shows the comparison between the measured peak heat flux in liquid helium and the well-known correlation in ordinary fluid. In **Fig.10**, Straub's summary of measurement results and Lienhard–Dhir correlation were also drawn [26]. Vertical axis is normalized value with the heat flux from Zuber's equation given by

$$q_{c\infty} = 0.131\rho_v^{0.5} h_{fg}\left[\sigma g(\rho_l - \rho_v)\right]^{0.25} \tag{6}$$

The horizontal axis is normalized radii defined by the following equation,

$$R' = R\sqrt{\frac{g(\rho_l - \rho_v)}{\sigma}} \tag{7}$$

Lienhard–Dhir correlation is expressed by combining Eq. 6 and Eq. 7.

$$q_{cr} = 0.94 q_{c\infty} R'^{-0.25} \tag{8}$$

Figure 10 indicates that boiling in He I obey the universal correlation together with the other fluids. On the other hand, boiling in He II is much different from the correlation. Thus, it can be said that the boiling mechanism should be unique in the case of He II because nucleation boiling state is absent.

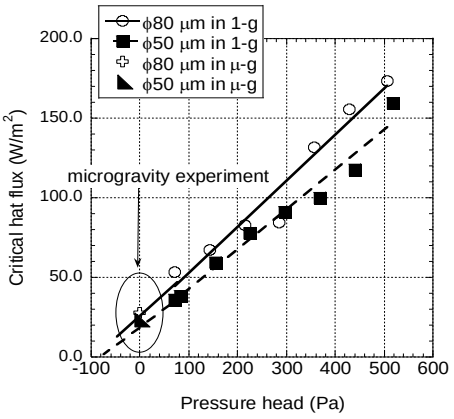

Fig. 8 Dependence of critical heat flux of thin wires, 80 μ m and 50 μm in diameter on hydrostatic pressure of He II with T_b = 1.9 K. The solid line and the dotted line represent fitting curves for the experimental results in earth gravity [24].

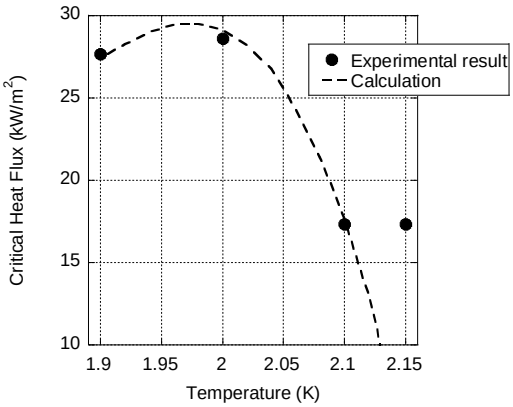

Fig. 9 Comparison of temperature dependence of critical heat flux under microgravity condition with Eq. (5). The diameter of the heater wire is 80 μm [24].

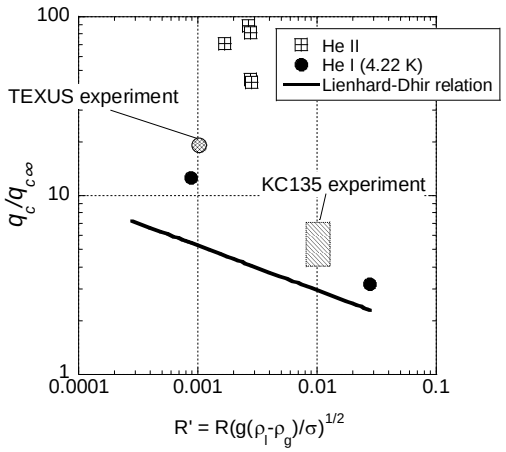

Fig. 10 Comparison of the critical heat flux of wires from Helium experiment with previously obtained results [26] and from Lienhard–Dhir correlation [24].

4. Heat Transfer Across Liquid-Vapor Interface (Recovery Heat Flux)

The recovery heat flux when the vapor film vanishes has also been investigated by using the drop tower [27-29]. Because of short time duration of microgravity, the hysteresis curve of boiling heat transfer could not be obtained during dropping. The heat transport across liquid-vapor interface was investigated on the basis of the visualization results because the recovery heat flux must be the maximum heat flux across the liquid-vapor interface when the vapor radius decreases to the radius of heater surface.

The heat transfer across the liquid-vapor interface were calculated by subtracting the consumption of vaporization calculated by the derivative of vapor volume and the latent heat from the total applied heat. In other expressions, the heat transport Q_i from the vapor-liquid interface and the residual heat was spent on evaporation. Thus, the time derivative of gas volume is calculated by the following equation

$$\frac{dV}{dt} = \frac{Q - Q_i}{\rho_v h_{fg}} \tag{9}$$

In this experiment all heater surface were completely dry-out. Thus, all heat from the heater wire through across vapor bubble by thermal conduction. Only heat transfer across the vapor-liquid interface can explain the vapor growth rate. **Figure 11** are typical visualization results of a single bubble growth from short heater of approximately 2 mm. **Figure 12** shows ~~a~~ typical measurement results of the vapor volume variation based on visualization results such as **Fig.11**.

These estimations were in good agreement with the calculations using the energy balance equation on the vapor-liquid interface, based on kinetic theory [30-32] as shown in **Fig.13**.

$$2\sqrt{\pi}\left(\frac{1-0.4\beta}{\beta}\right)j - \frac{4\sigma}{D}\sqrt{2R_{He}T_i} + \frac{\sqrt{\pi}}{4}q_i = 0 \tag{10}$$

Where T_i is the temperature at the interface (not the bath temperature). However, the relation $T_i \fallingdotseq T_b$ may be assumed due to negligibly small temperature difference between T_i and T_b because He II has extremely high thermal conductivity. The value of β was set to 0.72, according to the past research [33].

However, the experimental results are obtained during a transient process as shown in **Fig.13**. The further experiments were conducted using the high drop tower at ZARM (Center of Applied Space Technology and Microgravity) in Bremen [29]. The ZARM drop tower can provide up to 4.7 s of microgravity conditions. **Figure 14** shows the time variation of single bubble growth at several heat flux in 1.9 K He II bath. These results indicate that above equation (9) and (10) were in good agreement with the experiment results with the steady state estimation. This kind of visualization experiment can be conducted only in a microgravity environment. On ground gravity, the vapor bubble

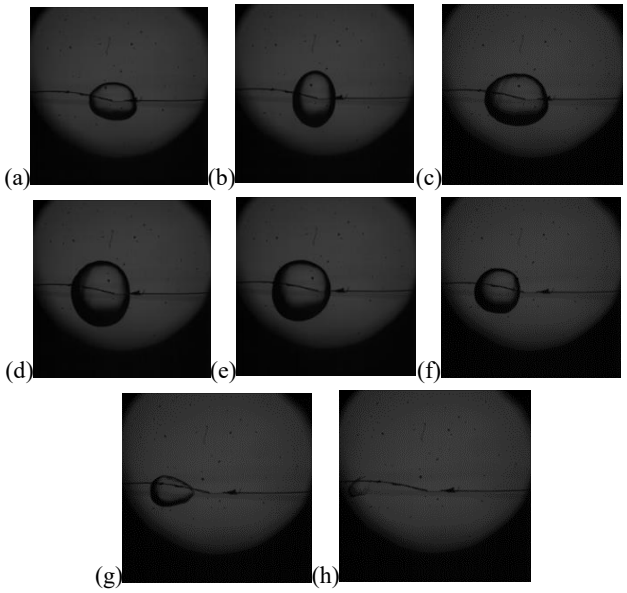

Fig. 11 A typical series of photographs of a single bubble growth and shrinking in He II under microgravity for 18.05 mW at 1.9 K (a) 0.089 s, (b) 0.193 s, (c) 0.297 s, (d) 0.401 s, (e) 0.504 s, (f) 0.608 s, (g) 0.712 s and (h) 0.816 s [27].

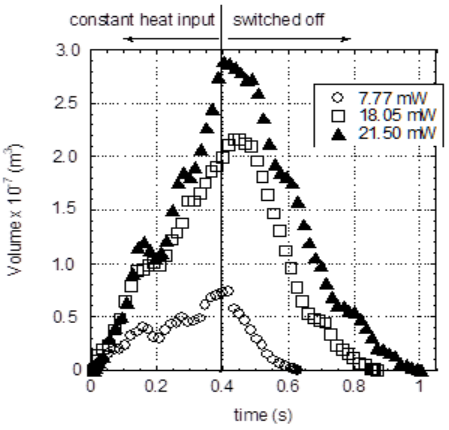

Fig.12 Time variations of bubble volume on several heat inputs for 0.4 s at the bath temperature T_b = 1.9 K, t = 0 s is the moment when heater switched on [26].

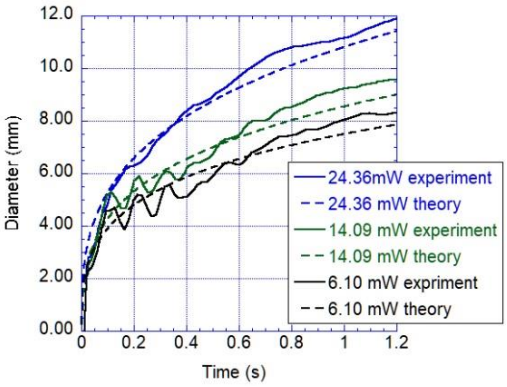

Fig. 13 Time variation of diameter of bubble growth for several heat inputs at T_b = 1.9 K at the drop tower of AIST.

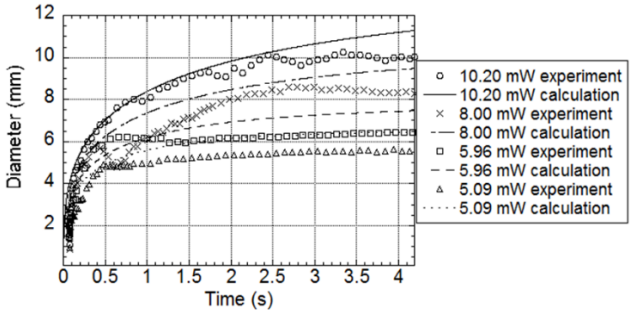

Fig.14 Time variation of diameter of bubble growth for several heat inputs at T_b = 1.9 K at ZARM drop tower [29].

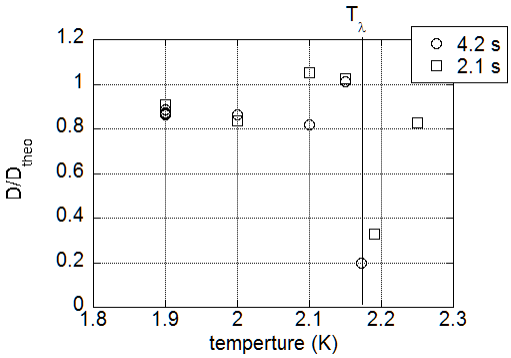

Fig.15 Temperature dependence of the ratio between experimental results and calculation results at the time t = 4.2 s and 2.1 s [29].

is too small, and the motion is too fast to observe time variation of bubble growth. These good agreements can be seen for wide temperature range even including He I temperatures as shown in **Fig.15**. This good agreement with the kinetic theory results can be extended to explain also the past experimental results [16]. The heat transfer across He II-vapor interface is found to be very small so that the bubble shrinking rate may be considered also small. In the past experimental results of the recovery heat flux were always measured smaller than the prediction because the vapor bubble has not reached steady state in limited time duration of microgravity.

However, near the temperature of He II-He I phase transition (which is called the lambda temperature), the vapor growth is much smaller than the predicted value, which means a large heat transfer occurred. This discrepancy may indicate the anomaly in physical properties at He II-He I phase transition. In fact, several properties are changing drastically around He II-He I phase transition. More precise experiments are required.

It should be added that this type of experiment is not possible in the other fluids because the heat transfer is too small. In He II experiment under microgravity, the situations are quite suitable to measure the heat transfer across the interface. The vapor density is small so that the bubble is rather large enough to measure and the viscosity is quite small. The latent heat is also

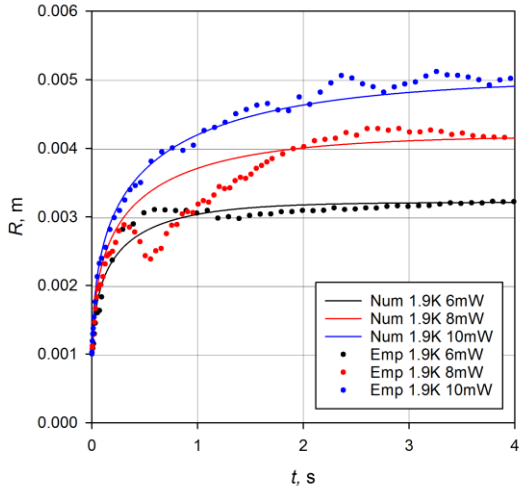

Fig.16 Experimental results of bubble radius growth and the precise calculation at T_b = 1.9 K [36].

small. Furthermore, the temperature distribution is negligibly small throughout He II.

5. Numerical Studies

The numerical studies of the boiling have been carried out by a Russian group [34, 35]. However, they did not have any experimental results to validate their numerical results. On the other hand, Grunt *et al.* [36] have conducted a numerical study based on experimental data [29] relying on the Russian group's achievement [34, 35]. This numerical calculation was more precise than the previous results mentioned above based on Eq. (9) and (10). In this study, several terms neglected in the previous study were taken into account, such as Rayleigh-Plesset equation, the transient heat transfer to develop temperature distribution. **Figure 16** shows the comparison between the experimental and the numerical results. The precise numerical calculation can predict the vapor bubble growth quite well through the previous simple analysis [29]. The study also indicated that the simple analysis is significant to explain dominant heat transfer mechanism. However, even these numerical studies [35, 36] have not succeeded in the explaining the anomaly near the temperature of He II- He I phase transition. The precise numerical study has attempted to discuss about several factors in detailed, however the accuracy of the experimental results was not enough to verify their prediction.

6. Summary and Open Issues

Several microgravity experiments of boiling heat transfer in He II have revealed the following heat transfer mechanism but have still left some open issues which must be solved for future advanced application in space.

The findings are summarized below.

1) The peak and the recovery heat flux of boiling can be extrapolated from the correlation on hydrostatic pressure head which can be provided on ground gravity experiments.

2) The van der Waals force plays a significant role in determining the peak heat flux. The extended Gorter-Millink equation taking into account the van der Waals force can successfully predict the peak heat flux.

3) The heat transfer across the He II-vapor interface can be calculated by the simple equation on the basis of the kinetic theory. The results of visualization study conducted in microgravity environment can directly give the estimation of heat transfer across He II- vapor interface directly in microgravity environment.

However, the several open issues still remain.

1) The anomaly around the lambda temperature of He II-He I phase transition could not be explained.

2) The model of the transient heat transfer including He II-He I phase transition was not described.

All experimental studies of He II heat transfer under microgravity condition have been carried out in saturated vapor pressure condition. Furthermore, the transient heat transfer accompanying with pressurized He II should be investigated under microgravity experiment when the application of the thermal storage tank of He II will be developed.

Acknowledgments

The author would like to express his appreciation for the fruitful discussions with Prof. M. Murakami and Dr. Kimura.

References

1) S.W. Van Sciver: Helium Cryogenics, 2nd Edition, Springer (2012).
2) S. W. Van Sciver: Advances in Cryogenic Engineering, **27** (1982) 375.
3) A. Sato, T. Miki, T. Kiyoshi, F. Matsumoto, H. Nagai, H. Wada, S. Ito, M. Yoshikawa, Y. Kawata and S. Fukui: Proc. of ICEC, **18** (2000) 407.
4) R. Maekawa, S.W. Van Sciver and H.J. Schneider-Muntau: Cryogenics, **32** (1992) 283.
5) L. Evans: IEEE Transactions on Applied Superconductivity, **10** (2000) 44.
6) G. Claudet, G. Bon Mardion, B. Jager and G. Gistaut: Cryogenics, **26** (1986) 443.
7) M. Hirabayashi, K. Narasaki, S. Tsunematsu, Y. Kimura, S. Yoshida, H. Murakami, T. Nakagawa,A. Ohnishi, T. Matsumoto, H. Kaneda, K. Enya, M. Murakami: Cryogenics, **48** (2008) 187.
8) R. Fujimoto, K. Mitsuda, N. Yamasaki, Y. Takei, M. Tsujimoto, H. Sugita, Y. Sato, K. Shinozaki, T. Ohashi, Y. Ishisaki, Y. Ezoe, M. Murakami, S. Kitamoto, H. Murakami, T. Tamagawa, M. Kawaharada, H. Yamaguchi, K. Sato, J. Herder: Cryogenics, **50** (2010) 488.
9) M.J. DiPirro, P.J. Shirron and J.G. Tuttle: Cryogenics, **34** (1994) 267.
10) J.H. Lee: Cryogenics, **30** (1990) 166.
11) L.C. Yang and P.V. Mason: Cryogenics, **20** (1980) 91.
12) S.W.K. Yuan and T.H.K. Frederking: Cryogenics, **27** (1987) 27.
13) M. Murakami, N. Nakaniwa, S. Hayakawa, T. Matsumoto, K. Noguchi, H. Murakami, K. Uyama and H. Nagano: Proc. of **9th** ICEC, (1982) 45.
14) P. Mason, D. Collins, D. Petrac, L. Yang, F. Edeskuty and K. Williamson: Proc. of **6th** International Cryogenic Engineering conf., (1976) 187.
15) K.D. Williamson, Jr., F.J. Edeskuty and J.F. Taylor: A rocket-borne, low Gravity Cryogenic Heat Transfer Experiment, AIAA-NASA/ASTM/TES, **7th** Space Simulation Conf., (1973).
16) T. Gradt, Z. Szücs, H.D. Denne and G. Klipping: Advances in Cryogenic Engineering, **31** (1986) 499.
17) J. Lipa, D.R. Swanson, J.A. Nissen and T.C.P. Chui: Cryogenics, **34** (1994) 341.
18) S. Takada, M. Murakami and N. Kimura: Advances in Cryogenics Engineering, **55 B** (2010) 1335.
19) M. Nozawa, N. Kimura, M. Murakami and S. Takada: Cryogenics, **49** (2009) 583.
20) S. Takada, M. Murakami, N. Kimura and B. Koh: Proc. of **23rd** ICEC, (2011) 325.
21) R.Z. Wang and P. Zhang: Cryogenics, **38** (1998) 701.
22) N. Kimura, S. Takada, S. Gotoh, H. Kawamata, M. Iida, M. Murakami, H. Nagai and M. Mamiya: Cryogenics, **51** (2011) 70.
23) S. Takada, N. Kimura, M. Mamiya, M. Nozawa, T. Okamura and M. Murakami: Proc. of **24th** ICEC, (2013)119.
24) S. Takada, N. Kimura, M. Mamiya, H. Nagai, T. Okamura, M. Murakami and M. Nozawa: Int. J. Microgravity Sci. Appl., **31** (2014)186.
25) S.C. Soloski and T.H.K. Fredeking: Int. J. Heat Mass Transf., **23** (1980) 437.
26) J. Straub, M. Zell and B. Vogel: Proc. of the First European Symposium, Fluid in Space, (1992) 269.
27) S. Takada, N. Kimura, M. Murakami and T. Okamura: IOP Conf. Series, Materials Science and Engineering, **101**, conf. 1 (2015) 012163.
28) S. Takada, N. Kimura, M. Murakami and T. Okamura, Physics Procedia, **67** (2015) 591.
29) S. Takada, N. Kimura, S. Pietrowicz, K. Grunt, M. Murakami and T. Okamura: Cryogenics, **89** (2018) 157.
30) Y. Ametitov: Cryogenics, **23** (1983) 179.
31) A.P. Kryukov and S.W. Van Sciver: Cryogenics, **21**(1981) 525.
32) D.A. Labuntzov and Y. Ametitov: Cryogenics, **19** (1979) 401.
33) M. Murakami, T. Furukawa, M. Maki and J. Fujiyama: Exp. Therm. Fluid Sci., **26** (2002) 229.
34) I.M. Dergunov, A.P. Kryukov and A.A. Gorbunov: J. Low Temp. Phys., **119** (2000) 403.
35) P.V. Khurtin and A.P. Kryukov: J. Low Temp. Phys., **119** (2000) 413.
36) K. Grunt, M. Lewkowicz, S. Pietrowicz, S. Takada, N. Kimura and M. Murakami: Int. J. Heat Mass Transf., **134** (2019) 1073.